

Electrical breakdown properties in neon gas mixed with xenon

Han S. Uhm, Eun H. Choi*, Guansup Cho* and Ki W. Whang**

Department of Molecular Science and Technology, Ajou University, Suwon 442-749, Korea

**Department of Electrophysics/PDP Research Center, Kwangwoon University, Seoul 139-701, Korea*

***School of Electrical Engineering, Seoul National University, Seoul 151-742, Korea*

(Received November 27, 2000)

Abstract –The paper investigates electrical discharge properties in neon gas mixed with xenon. The breakdown temperature T_b and voltage V_b are obtained in terms of the gas mixture ratio χ . It is shown that the breakdown voltage decreases, reaches the minimum value at $\chi = 0.02$ and then increases again, as the mixture ratio χ increases from zero to unity. Therefore, mixing the neon gas with a few percent of xenon is the most beneficial to reduce the breakdown voltage. Plasma density at breakdown in neon gas mixed with xenon is described in terms of the gas mixture ratio. The optimum value of mixture ratio for highest plasma density is found to be $\chi_m = 0.03$. A preliminary experiment of AC-PDP is carried out for neon gas mixed with a few percent of xenon to verify some of the theoretical models. The experimental data agree qualitatively well with theoretical predictions.

I. Introduction

The first issue to generate plasma easily is reduction of the breakdown voltage. We consider the electrical discharge system in high-pressure inert-gas in connection with its applications to the plasma display panel (PDP) [1-3]. Reduction of the breakdown voltage in a low pressure gas by the Penning effects was reported in previous literature [4], where one hundredth of one percent of argon gas is mixed with neon. However, the plasma display panel is operated at high-pressure gas and the breakdown voltage reduction in a mixed gas is mostly accomplished by collision-frequency decrease. The UV light emitted from xenon discharge plasma is converted into fluorescence which provides an image on TV screen. The discharge plasma is generated by the electrical breakdown. Reduction of the discharge voltage is therefore the key element in enhancing the electrical efficiency of PDP. The electrical efficiency enhancement in turn prolongs the panel lifetime. Size of xenon atoms is relatively large so that electrons in the plasma are highly collisional. Therefore, electron mean free-path is small in xenon gas, requiring high breakdown voltage. Plasma generation in a mixture of xenon and light-atom gases may not need high breakdown voltage. We therefore investigate electrical discharge properties in a mixed gas.

Properties of breakdown voltage in a mixed gas are investigated in Sec. II based on Townsend criterion. The ionization energy of heavy atoms is usually low, although their atomic size is large. Plasmas are generated from ionization of neutrals by the impact ionization of electrons, which have their kinetic energy higher than ionization energy. Electrons with energy higher than ionization energy collide with neutrals, ionizing, and creating additional electrons and ions. Therefore, it is easy to ionize neutrals with less ionization energy. Meanwhile, electron energy-gain in large-size neutrals is difficult due to small mean free-path. The electrons can easily get their kinetic energy in a light-atom gas mixed with heavy atoms. Once having enough kinetic energy, they collide with heavy atoms of low ionization energy, producing additional electrons and ions. The breakdown temperature T_b [Eq. (6)] and voltage V_b [Eq. (10)] are obtained in terms of the gas mixture ratio χ in Sec. II. We investigate electrical breakdown properties in neon gas mixed with xenon. It is shown that the electron breakdown-temperature T_b decreases monotonically as the mixture ratio χ increases. On the other hand, the breakdown voltage decreases, reaches the minimum value at $\chi = 0.02$ and then increases again, as the mixture ratio χ increases from zero to unity. We have carried out a preliminary experiment of

AC-PDP to verify some of the theoretical models in this paper. The experiment is carried out for neon gas mixed with a few percent of xenon. Both theory and experiment show that the minimum breakdown-voltage occurs around the mixture ratio of $\chi \approx 0.02$. The experimental data agree qualitatively well with theoretical predictions.

Properties of the plasma density at breakdown in a mixed gas are investigated in Sec. III based on the electron rate-equation. The estimate of ion density is carried out and is shown that ions consist mostly of the heavy atoms due to low ionization energy and large ionization cross section. An expression of plasma density [Eq. (29)] is obtained in terms of the gas mixture ratio. It is also found from Eq. (29) that the maximum plasma density occurs at the mixture ratio $\chi = \chi_m = T_0/\zeta\epsilon_X$ [Eq. (31)] where T_0 is the electron breakdown-temperature of a single-species gas, ζ is the relative ratio of the scattering cross section and ϵ_X is the ionization energy of heavy atoms. As an example, we consider plasma generation in neon gas mixed with xenon. The parameter ζ in this mixed gas is $\zeta = 11$. Typical value of the single-species temperature T_0 in this mixed gas is $T_0 = 3.9$ eV. The ionization energy of xenon is $\epsilon_X = 12.2$ eV. Substituting these numbers into Eq. (31), we find that optimum value of the mixture ratio for highest plasma density is $\chi_m = 0.03$ for neon gas mixed with xenon.

II. Breakdown Voltage in a Mixed Gas

The electron temperature T_b at breakdown is obtained from sparking criterion [5] (also known as the Townsend criterion)

$$\alpha d = \ln(1 + 1/\gamma) \quad (1)$$

in a gas without electron attachment where γ represents the secondary electron-emission coefficient (also known as Townsend's second ionization coefficient [5]) of low energy ion bombardment at the cathode. The ionization coefficient α in Eq. (1) is known as Townsend's first ionization coefficient, and is defined as the number of ionizing collisions made on the average by an electron as it *travels one centimeter in the direction of the electric field E* . The electron travels with the drift velocity v_d in the direction of the electric field E . The ionization rate α_{th} in unit time of neutrals by plasma electrons is expressed as

$$\alpha_{th}(T) = n_n \int_0^\infty \sigma(\epsilon) v g(\epsilon) d\epsilon \quad (2)$$

where v is velocity of plasma electron corresponding to the electron energy of ϵ , $\sigma(\epsilon)$ is the ionization cross section of neutrals by electrons and n_n is the neutral density that is 2.5×10^{19} particles per one cubic-centimeter at one atmospheric pressure with room temperature. Therefore, the ionization coefficient α in Eq. (1) for unit length is related to the ionization rate α_{th} in Eq. (2) for unit time by $\alpha = \alpha_{th}/v_d$. The energy distribution function $g(\epsilon)$ of plasma electrons in Eq. (2) can be a complicated function, depending on individual experimental conditions. However, for the time being, we assume a Maxwellian distribution where the electron temperature T is related to the mean electron energy $\langle \epsilon \rangle$ by $\langle \epsilon \rangle = 3T/2$. The electron temperature T is typically in units of eV. We have also assumed that the breakdown electric field E in Eq. (1) is provided by two planar electrodes separated by distance d in units of cm.

Bulk plasma experiments were conducted for various neutral gases. The ionization cross section $\sigma(\epsilon)$ of these neutrals versus electron energy ϵ has been well documented. For example, the ionization cross section $\sigma(\epsilon)$ of argon neutrals by electrons is documented experimentally in Ref. 6. The maximum ionization cross-section occurs near the electron energy $\epsilon = 100$ eV for most of the gas species. Typical ionization energy ϵ_i is about 15 eV for these gases. The ionization energy of argon atoms is $\epsilon_i = 15.76$ eV. For electron temperature T considerably less than the ionization energy ϵ_i , the ionization coefficient $\alpha = \alpha_{th}/v_d$ in Eq. (1) can be obtained from Eq. (2) and is approximately given by

$$\alpha(T) = 2n_n \frac{v_{th}}{v_d} \frac{q}{\sqrt{\pi}} (\epsilon_i + 2T) \exp\left(-\frac{\epsilon_i}{T}\right) \quad (3)$$

where q is the increase rate of ionization cross section and v_{th} is the thermal velocity. The increase rate q is in units of cm^2/eV and the energy ϵ_i and temperature T are in units of eV. The increase rate q represents the profile of the ionization cross section, including its size. An equation similar to Eq. (3) was first obtained in Ref. 7. The ionization coefficient in Eq. (3) is a good approximation for the neutrals ionized by plasma electrons with a temperature less than ionization energy ϵ_i . Note that the electron temperature T in Eq. (3) is usually much less than the ioniza-

tion energy ϵ_i . The ionization coefficient α in Eq. (3) is proportional to the neutral gas pressure (n_n). We also remind the reader that the ionization coefficient in Eq. (3) is obtained under the assumption of Maxwellian energy distribution of electrons.

Electrons in the presence of a strong electric field are accelerated, gaining kinetic energy. Plasma is generated by the electron impact ionization, where high-energy electrons collide and ionize neutrals in the discharge gas, creating additional electrons and ions. Thus, the ionization produces additional electrons. The ionization coefficient α of the discharge gas is also expressed as [8]

$$\alpha(E/p) = hp \exp\left(-g \frac{p}{E}\right), \quad (4)$$

where E is the electric field in units of volts/cm, and p is the gas pressure in units of atmosphere. The coefficients h and g are obtained from experimental data for a specified gas. Equation (4) describes the discharge experiments reasonably well for a certain range of E/p . For example, the constants [9] h and g of air are given by $h = 3.5 \times 10^3 \text{ cm}^{-1}$ and $g = 1.65 \times 10^5 \text{ volt/cm-atm}$, which are valid only for the electric field satisfying $1.25 \times 10^3 \text{ V/cm-atm} < E/p < 2 \times 10^5 \text{ V/cm-atm}$. The breakdown field of air is about $E/p = 3 \times 10^4 \text{ V/cm-atm}$, which is well inside the validity range. Equation (4) is the ionization coefficient used in most of the discharge experiments [5, 8].

Several points are noteworthy from Eqs. (3) and (4). First, the ionization coefficient in Eq. (3) obtained theoretically must be identical to the empirical expression in Eq. (4) of the coefficient. The functional forms of the two expressions are obviously identical to each other. Remember that Eq. (3) has been obtained under the assumption of the Maxwellian distribution. Therefore, the Maxwellian energy distribution is a reasonable approximation for electrons in a relatively high-current environment corresponding to electrical breakdown. The mean energy of electrons in a positive column of an electrical discharge was measured in previous experiments [4] and the experimental data in neon gas are in good agreement with the calculation on the basis of the Maxwellian distribution. Second, the independent variable in Eq. (3) is the electron temperature T , whereas the independent variable in Eq. (4) is E/p . We therefore recognize that the electron temperature T in Maxwellian distribution is proportional to the

parameter E/p . Third, neglecting the electron temperature T in comparison with the ionization energy ϵ_i , the constant of the ionization coefficient in Eq. (3) is uniquely proportional to the neutral density n_n which is in turn proportional to the pressure p in Eq. (4).

Assuming that the gas consists of two species X and N, the ionization coefficient for this mixed gas can be expressed as

$$\alpha(T) = 5 \times 10^{19} \frac{p}{\sqrt{\pi}} \frac{v_{th}}{v_d} [(1 - \chi) q_N (\epsilon_N + 2T) \exp\left(-\frac{\epsilon_N}{T}\right) + \chi q_X (\epsilon_X + 2T) \exp\left(-\frac{\epsilon_X}{T}\right)], \quad (5)$$

where the symbol χ denotes the normalized mixture ratio of the gas species X. As an example of Eq. (5), we have obtained the ionization coefficient of air consisting of nitrogen and oxygen molecules with the ratio of four to one. The ionization coefficient of air predicted by Eq. (5) agrees remarkably well with data obtained experimentally [10]. Substituting Eq. (5) into Eq. (1), the electron temperature T_b at the breakdown is obtained from

$$5 \times 10^{19} \frac{v_{th}}{v_d} \frac{pd}{\sqrt{\pi}} \left[(1 - \chi) q_N \epsilon_N \exp\left(-\frac{\epsilon_N}{T_b}\right) + \chi q_X \epsilon_X \exp\left(-\frac{\epsilon_X}{T_b}\right) \right] = \ln\left(1 + \frac{1}{\gamma}\right) \quad (6)$$

where we have neglected the terms proportional to $2T_b$ in comparison with the ionization energies. Once the gas mixture ratio χ is known, the electron temperature T_b at the breakdown can be determined from Eq. (6) in terms of the parameter pd .

The mean free path λ of electrons in the mixed-gas molecules is inversely proportional to the product of scattering cross section and neutral number density. That is

$$\frac{1}{\lambda} = [\sigma_N(1 - \chi) + \sigma_X \chi] n_n = 2.5 \times 10^{19} [\sigma_N(1 - \chi) + \sigma_X \chi] p \quad (7)$$

where σ_N and σ_X denote the scattering cross sections of species N and X, respectively, and p is the gas pressure in units of atmosphere. The electrons are accelerated by the electric field E , gaining their kinetic energy of λeE before they collide with neutrals. These slow electrons are scattered isotropically in collisions with molecules, thermalizing their gained energy. This process repeats until they establish their

temperature $T = \xi \lambda e E$, where ξ is the thermalization form factor of electron energy [10]. Remember that the electron temperature in Maxwellian distribution is proportional to E/p and the mean free path λ is inversely proportional to pressure p . Therefore, the electron temperature is proportional to the product of the mean free path λ and the electric field E , and is expressed as

$$\frac{1}{T} = 2.5 \times 10^{19} \frac{\sigma_N p}{\xi E} [1 + \zeta(T) \chi], \quad (8)$$

where the relative ratio ζ of the scattering cross section is defined by

$$\zeta(T) = \frac{\sigma_X - \sigma_N}{\sigma_N} \quad (9)$$

The electron temperature in Eq. (8) is well known and corresponds to the approximation for the mean free path. The approximation for the mean free path in Eq. (8) corresponds actually to the Druyvesteyns energy distribution, as shown in Ref. 11. Meanwhile, we have used the Maxwellian distribution in obtaining Eq. (3) for simplicity of subsequent analysis. The Maxwellian distribution originates from a constant value of the free collision-frequency for electrons. However, the Maxwellian approximation predicts a reasonably correct ionization coefficient for many applications, as will be seen later. The form factor ξ can be found by properties of gas species and by thermalization properties of electrons. The energy distribution of low-current electrons has been shown to be a non-Maxwellian distribution [4], which is a function of only the parameter $\lambda e E$. Therefore, the mean energy [4] of the low-current electrons is also proportional to the parameter $\lambda e E$.

The breakdown voltage $V_b = Ed$ is calculated from Eq. (8) and can be expressed as

$$\xi V_b = 2.5 \times 10^{19} \sigma_N T_b [1 + \zeta(T_b) \chi] p d, \quad (10)$$

where the electron temperature T_b is obtained from Eq. (6) in terms of the parameter $p d$. Equation (10), together with Eq. (6), is one of the main results of this article and can be used to obtain the breakdown voltage in a mixed gas. The breakdown voltage V_b can be considerably reduced by an appropriate choice of the gas species whose ionization energies and collisional cross sections can provide optimum condition. For completeness of analysis, we estimate

the ratio v_{th}/v_d of the thermal velocity to the drift velocity for electrons. The electron drift velocity in weakly ionized plasmas is given by [12, 13]

$$v_d = \frac{\lambda e E}{m v_{th}}, \quad (11)$$

for $v_{th} \gg v_d$ typical in discharge plasmas. Here m is the electron mass. Making use of the electron temperature $T = \xi \lambda e E = (1/2) m v_{th}^2$ and eliminating the electric field in Eq. (11), we obtain $v_{th}/v_d = 2\xi$. Therefore, the thermalization form factor ξ is one half of the ratio v_{th}/v_d of the thermal velocity to the drift velocity.

As an example, we consider neon gas mixed with xenon. The neon gas mixed with a few percent of xenon is used in the plasma display panel (PDP) for apparent reasons shown later. We assume that the subscript N and X in Eq. (6) represent the neon and xenon species. The increase rate q_N and q_X of ionization cross section for neon and xenon are given by [6] $q_N = 1.2 \times 10^{-18} \text{ cm}^2/\text{eV}$ and $q_X = 3.12 \times 10^{-17} \text{ cm}^2/\text{eV}$, respectively. The ionization energies for these gas species are given by [6] $\epsilon_N = 21.5 \text{ eV}$ and $\epsilon_X = 12.2 \text{ eV}$. Making use of the power parameter a defined by $a = \epsilon_N/\epsilon_X$ and carrying out a straightforward calculation, we obtain

$$\left[(1 - \chi) U^a + \frac{q_X \epsilon_X}{q_N \epsilon_N} \chi U \right] = \frac{\sqrt{\pi} \ln(1 + 1/\gamma)}{10^{20} q_N \epsilon_N \xi p d}, \quad (12)$$

from Eq. (6), where the function U is defined by

$$U = \exp\left(-\frac{\epsilon_X}{T_b}\right) = \exp\left(-\frac{12.2}{T_b}\right), \quad (13)$$

for xenon gas. Once value of the unknown U is found, the corresponding temperature can be obtained from Eq. (13).

The thermalization form factor ξ is not known for neon and xenon. The thermalization form factor [10] of air consisted of diatomic molecules is found to be $\xi = 3$. We expect that thermalization form factor for majority of experimental gas at high pressure, where the electron temperature is about 1 eV, is in the range of $2 < \xi < 6$. However, the electron breakdown-temperature in Eqs. (12) and (13) is a logarithmic dependence of the form factor ξ . Therefore, corrections of electron temperature associated with a correct value of the form factor is negligibly small. As an example, we consider PDP cells, assuming that the

secondary electron-emission coefficient γ at the cathode is $\gamma=0.2$. Assuming that the thermalization form factor of neon is $\xi = 3$, the right-hand side of Eq. (12) is calculated to be 3.8×10^{-3} for $p = 1$ atmosphere and $d = 0.1$ cm, which are typical to PDP applications. The number 3.8×10^{-3} is a very small value, thereby generating a small value of U in Eq. (12). Note that the parameter $q_X \epsilon_X / q_N \epsilon_N$ in Eq. (12) is $q_X \epsilon_X / q_N \epsilon_N = 12.8$ which is a considerably large value. Therefore, the term proportional to χU in the left-hand side of Eq. (12) dominates over the term proportional to U^a even for a relatively small value of the mixture ratio χ , where the power parameter $a = 1.77$. We remind the reader that the term proportional to χU in the left-hand side of Eq. (12) originates from the contribution of xenon ionization, whereas the term proportional to $U^{1.77}$ originates from neon contribution. Ions are mostly generated from the ionization of xenon due to a low ionization energy, as expected. Therefore, the electron breakdown-temperature T_b is mostly decided by the xenon ionization energy. The typical electron energy $\langle \epsilon \rangle$ at breakdown is about $\langle \epsilon \rangle \approx 3.75$ eV corresponding to the breakdown temperature $T_b = 2.5$ eV. The collisional cross sections of neon [14] and xenon [15] gases for the electron energy of $\langle \epsilon \rangle = 3.75$ eV are given by $\sigma_N = 2.5 \times 10^{-16}$ cm² and $\sigma_X = 3 \times 10^{-15}$ cm², respectively. Therefore, the parameter ζ defined in Eq. (9) is given by $\zeta = 11$ for $T_b = 2.5$ eV. The breakdown voltage V_b in Eq. (10) is proportional to the collisional cross section σ_N of neon for a small value of mixture ratio χ . Although the ions are generated from xenon gas, the breakdown voltage in Eq. (10) is mostly determined from collisional cross section of neon, which is one-twelfth of collisional cross section of xenon for the electron energy of $\langle \epsilon \rangle = 3.75$ eV. In this regard, the breakdown voltage can be considerably reduced by mixing neon with xenon.

Substituting proper numbers into Eqs. (12), (13) and (10) for neon gas mixed with xenon, we obtain

$$[(1 - \chi)U^{1.77} + 12.8\chi U] = 3.8 \times 10^{-3} \quad (14)$$

$$T_b = \frac{12.2}{\ln(1/U)}, \quad (15)$$

and

$$\Gamma_b = \frac{\xi}{pd} V_b = 6.25 \times 10^3 T_b (1 + 11\chi), \quad (16)$$

where the normalized discharge voltage Γ_b is in units of volt and the anode-cathode distance d is in units of cm. The solution U in Eq. (14) decreases drastically from $U = 0.0421$ to $U = 2.97 \times 10^{-4} / \chi$ as the mixture ratio χ increases from zero to unity. Therefore, the electron breakdown temperature T_b decreases monotonically from $T_b = 3.86$ eV to $T_b = 1.5$ eV as the mixture ratio χ increases from zero to unity. As mentioned earlier, value of the solution U is much less than unity.

In order to verify the theoretical model in Eq. (10) for the breakdown voltage, we have carried out a preliminary experiment of AC-PDP, where three-electrodes system is used. Fig. 1 shows the cross sectional view of an AC-PDP cell structure. The transparent electrodes X and Y patterned by photolithography are covered with a dielectric layer whose thickness is about 30 μm and are parallel to each other in front glass, which is facing toward viewer and is protecting PDP discharge system. A MgO protective layer is deposited over the dielectric layer by electron-beam evaporation method with 0.5 μm in thickness. This MgO layer protects dielectric layer from charged particles in the discharge plasma. The sustaining discharge in the AC-PDP occurs between the parallel sustaining-electrodes X and Y in row. These electrode width is kept to be 300 μm , while gap distance between electrodes varies from

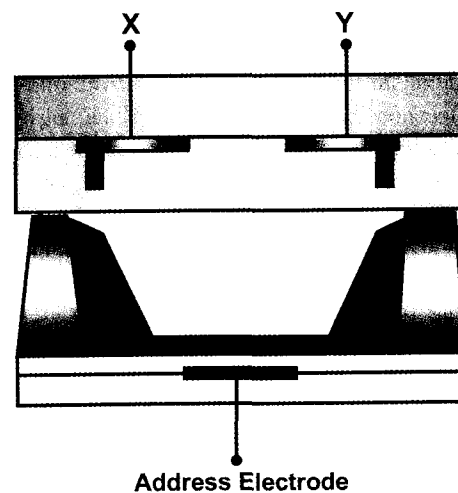


Fig. 1. Cross sectional view of an AC-PDP cell structure. The electrodes X and Y are covered with a dielectric layer whose thickness is about 20 μm and are parallel to each other in front glass.

50-200 μm for optimum efficiency of PDP operations. The distance between each pairs of these electrodes is 1080 μm . Therefore, the discharge spaces of the pair electrodes are parallel to the electrodes in row and are separated from each other by 1080 μm . The address electrode of 100 μm in width and the barrier rib of 130 μm in height are located beyond the dielectric layer and are aligned perpendicular to the sustaining electrodes, although they are appeared to be parallel in Fig. 1 for purpose of presentation. The barrier ribs are parallel to the address electrodes in column, subdividing the discharge space in row and providing isolated discharge cells. In other word, the 1080 μm spacing between rows of discharge space and the barrier ribs in column provide a full array of isolated discharge cells. The sustaining electrodes in row and address electrodes in column may also turn on and off the electrical discharge for each cells. However, initiation and turning-off signal of the discharge is fed by the address electrode, together with sustaining electrodes. Voltage of the address electrode has been kept to be a half of the sustaining voltage difference. In the experiment, a square voltage pulse with risetime of 150 ns and 40% duty ratio is applied between the two sustaining electrodes with fixed driving frequency of 50 kHz. The neon (Ne) is used as a main filling gas, and a small amount of xenon gas is introduced.

Note from Fig. 1 that the anode and cathode are in a coplanar alignment in PDP experiment. Therefore, they do not see each other. On the other hand, we have assumed that the anode and cathode plane-electrodes in the theory face each other with the gap distance of d . The essential parameter governing discharge mechanism is the electric field, although we have introduced the breakdown voltage for convenience. The breakdown electric field is obtained from Eq. (10), where the breakdown voltage can be divided by the anode-cathode gap d . We also note from Eq. (27) that the single-species temperature T_0 at breakdown is also defined by the electric field. Therefore, we conclude that information of the effective electric field inside the discharge space is needed for understanding discharge behavior. Distance of the anode-cathode gap for plane-electrodes facing each other is d . However, the effective distance between the anode-cathode gap in a coplanar geometry of PDP is the distance along the electric field-line from

anode to cathode. This effective distance may vary from point to point over the anode surface, where the field lines start. Therefore, we must find the average value $\langle d \rangle$ of the effective distance. The electric field inside a dielectric material may also depend on the dielectric constant. For example, the electric field perpendicular to the dielectric surface is not continuous at the surface, thereby not penetrating into the dielectric material with large dielectric constant [16]. This dielectric material also modifies the effective gap distance represented by d in Eq. (6), which determines the electron temperature T_b . The breakdown temperature T_b in Eq. (6) is a logarithmic dependence of the effective gap distance $\langle d \rangle$. Corrections of electron temperature associated with a correct value of the effective gap distance can be small due to the logarithmic dependence. The electron temperature in Eq. (10) is a decreasing function of the mixture ratio χ . We therefore recognize from Eq. (10) that the optimum mixture ratio χ for minimum breakdown field is almost independent of the effective gap distance. We also note from Eqs. (29) and (30) that the optimum mixture ratio in Eq. (31) for highest plasma density is also valid for curved field lines. However, the single-species temperature T_0 in Eq. (27) must be modified with a correct value of the effective gap distance $\langle d \rangle$.

Shown in Fig. 2 are plots of the breakdown voltage V_b versus the gas mixture ratio χ . The closed rectangular dots are experimental data obtained for $pd = 3.2$ Torr-cm. We remind the reader that although the anode-cathode gap is measured to be $d = 100$ μm

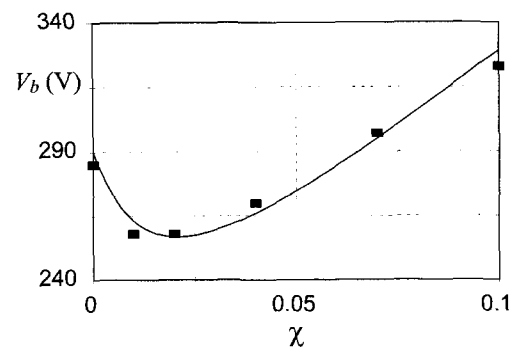


Fig. 2. Plots of the breakdown voltage V_b versus the gas mixture ratio χ . The closed rectangular dots are experimental data obtained for $pd = 3.2$ Torr-cm. The curve obtained from Eq. (10) is simply the least square fit of experimental data assuming $\xi/pd = 85$.

in coplanar geometry, the effective gap distance can be 500 μm or more, due to the geometrical effects of flat electrodes as shown in Fig. 1 and effects of the dielectric material over the electrodes. This is an approximate distance along the field lines started at the center of the anode surface. Note that discharge occurs in the space beyond dielectric material in Fig. 1. Therefore, the really effective value of parameter pd can be $pd = 16$ Torr-cm or more, even though the measured value is $pd = 3.2$ Torr-cm. The increase of effective value of parameter pd from $pd = 3.2$ Torr-cm to $pd = 16$ Torr-cm is due to the increase of effective gap distance from $d = 100$ μm to $d = 500$ μm . Note that $pd = 16$ Torr-cm is 0.022 atm-cm. The curve obtained from Eq. (10) in Fig. 2 is simply the least square fit of experimental data assuming $\xi/pd = 85$. Both the theory and experiment indicate that the minimum breakdown voltage occurs around the mixture ratio of $\chi \approx 0.02$. The breakdown voltage decreases to its minimum at $\chi \approx 0.02$ and then increases again, as the gas mixture ratio χ increases from zero to unity. We remind the reader that the mixture ratio $\chi = 1$ means the xenon gas only. Quantitatively comparing the theoretical result with experimental data may not be easy. However, the experimental data agree qualitatively well with theoretical predictions.

III. Plasma Density at Breakdown in a Mixed Gas

Plasma properties inside the discharge chamber can be described by numerically solving Boltzmann, moment and the Poisson equations for electrons and ions. This numerical calculation is very complicated because of seven coupled differential equations. However, we will obtain a simple analytical expression of plasma density and its generation by making use of quasi-neutrality of plasma region. The analytical description of plasma density is based on the electron moment equation

$$\frac{\partial n_e}{\partial t} + \frac{\partial}{\partial z}(v_d n_e) = \alpha v_d n_e - \frac{D}{\Lambda} - \alpha_r n_e^2, \quad (17)$$

where n_e is the electron density, v_d is velocity of the electron fluid element (or drift velocity), α is the ionization coefficient of neutrals by electrons. In Eq. (17), the term proportional to D is the diffusion loss

of electrons where Λ is the plasma linear scale, and the term proportional to α_r is the recombination loss of electrons. The characteristic ionization time of the first term in the right-hand side of Eq. (17) is $1/\alpha v_d$. The ionization time of argon plasma is 1 nanosecond for the electron temperature of $T = 2.5$ eV. Therefore, the discharge occurs within a few nanoseconds. On the other hand, the characteristic time of recombination is on the order of milliseconds. A typical discharge time of PDP cells is a fraction of a microsecond. Therefore, recombination in the discharge plasma in PDP cells is not important. Although the plasma linear scale Λ in a PDP cell is typically one millimeter or less, there is not enough time for a substantial diffusion loss. The diffusion loss can also be neglected if many cells discharge simultaneously. In this context, we may neglect the electron loss by the diffusion and recombination. The electron density analytically obtained from Eq. (17) in a high-pressure collision-dominated discharge for corona applications agrees well with numerical data obtained from seven coupled differential equations [17].

The electrons accelerated by the electric field may not necessarily have the Maxwellian energy distribution. However, as mentioned earlier, the slow electrons of a relatively high current moving through a high-pressure gas are scattered almost isotropically in collisions with neutral molecules, quickly establishing thermal equilibrium. Even for a small system like PDP cells, electrons collide with neutrals far more than 100 times before they reach the anode. As shown in Eq. (11), the electron drift velocity v_d in Eq. (17) is related to the thermal velocity, which is almost constant along the axial (z) direction. Substituting Eq. (5) into Eq. (17), the electron rate equation in a mixed gas is expressed

$$\begin{aligned} \frac{dn_e}{dt} &= \frac{\partial n_e}{\partial t} + v_d \frac{\partial n_e}{\partial z} \\ &= 5 \times 10^{19} n_e \frac{p}{\sqrt{\pi}} v_{th} \left[(1 - \chi) q_N \varepsilon_N \exp\left(-\frac{\varepsilon_X}{T}\right) \right. \\ &\quad \left. + \chi q_x \varepsilon_x \exp\left(-\frac{\varepsilon_N}{T}\right) \right] \end{aligned} \quad (18)$$

as where χ is the normalized mixture ratio of gas species X and where use has been made of the prop-

erty that the electron temperature is much less than the ionization energy. In obtaining Eq. (18), we have neglected the term proportional to $n_e (\partial v_d / \partial z)$ because of a quick thermalization of electrons at high pressure.

The voltage V over the gap between the anode and cathode is an increasing function of time t until it reaches the breakdown voltage V_b at the electrical breakdown-time $t = \tau_b$. Therefore, the voltage pulse before breakdown can be schematically expressed as

$$\frac{V}{V_b} = \left(\frac{t}{\tau_b} \right)^\eta, \quad (19)$$

where the power parameter η is related to the pulse risetime. The voltage over the gap increases very slowly at the beginning and then approaches the breakdown voltage quickly at the end of the pulse, if the power parameter η is much less than unity. On the other hand, the gap voltage approaches the breakdown voltage very quickly from the beginning, if the power parameter η is much larger than unity. The pulse rises more quickly, as the value of the power parameter η increases. In other words, the value of the power parameter η increases as the electrical pulse-risetime decreases. However, it is not necessary to find a detail information of the power parameter η for purposes of the present analysis. The electron temperature T increases with the electric field, as shown in Eq. (8). Therefore, the electron temperature $T = T(t)$ is an increasing function of time t , increasing from zero to the temperature T_b at breakdown, as time goes by. The electron temperature T is modeled to be

$$\frac{t}{\tau_b} = \left(\frac{T}{T_b} \right)^\eta. \quad (20)$$

Carrying out the time integration in Eq. (18) from zero to the breakdown time and changing the integration variable from time t to the temperature T , we obtain

$$\begin{aligned} Y(n_e, \chi) &= \ln \left[\frac{n_e}{n_0(z)} \right] \\ &= 2.1 \times 10^{27} \frac{P \tau_b}{\sqrt{\pi}} \left[(1 - \chi) q_N \varepsilon_N^{3/2} f\left(\frac{T_b}{\varepsilon_N}\right) + \chi q_X \varepsilon_X^{3/2} f\left(\frac{T_b}{\varepsilon_X}\right) \right] \end{aligned} \quad (21)$$

where the integral function $f(y)$ is defined by

$$f(y) = \eta y^{-\eta} \int_0^y x^{\eta-1/2} \exp\left(-\frac{1}{x}\right) dx. \quad (22)$$

In Eq. (21), the initial electron density $n_0(z)$ is, in general, assumed to be a function of its position z . Equation (21) with Eq. (22) is one of the main results of this section, and can be used to determine the plasma density at electrical breakdown for a broad range of system parameters, including the gas ionization cross-section (q), ionization energy (ε_i), gas pressure (p), discharge time (τ_b), the integral function $f(y)$ and the gas mixture ratio χ . The integral function $f(T_b/\varepsilon_N)$ and $f(T_b/\varepsilon_X)$ in Eq. (21) is described in terms of the electron temperature at breakdown and the power parameter η related to the electrical pulse-risetime as defined in Eq. (22).

The logarithm $Y(n_e, \chi)$ of the electron density n_e in Eq. (21) at the electrical breakdown is proportional to the breakdown time τ_b and the value of the integral function $f(T_b/\varepsilon_N)$ and $f(T_b/\varepsilon_X)$. The breakdown temperature T_b is usually much less than the ionization energies ε_N and ε_X . The integral function $f(y)$ has been investigated [18] in detail in terms of the normalized breakdown temperature y . As expected, the value of the function $f(y)$ increases significantly as the electron temperature at the breakdown increases. This increase is almost exponential for a small value of electron temperature characterized by $y \ll 1$. We also note from previous study [18] that value of the function $f(y)$ increases significantly as the power parameter η increases. For small values of the electron temperature satisfying $y \ll 1$, the integral function $f(y)$ is almost proportional to the power η . Value of the function inside the integration in Eq. (22) approaches zero very quickly, as the variable x approaches zero due to the exponential function in it. It is a slowly increasing function at a small value of x and then approaches $y^{\eta-1/2} \exp(-1/y)$ quickly at $x = y$. Therefore, we recognize the inequality

$$f(y) \leq \frac{1}{2} \eta \sqrt{y} \exp\left(-\frac{1}{y}\right), \quad (23)$$

which satisfies observation of numerical data [18] of Eq. (20). The inequality in Eq. (23) is obvious because the right-hand side of Eq. (23) is area of the triangle from $x = 0$ to the upper limit of integration $x = y$.

Substituting Eq. (23) into Eq. (21), the logarithm $Y(n_e, \chi)$ of the plasma density is approximately expressed as

$$Y(n_e, \chi) \leq 10^{27} \frac{P \tau_b}{\sqrt{\pi}} \sqrt{T_b} \eta \chi q_X \epsilon_X \exp\left(-\frac{\epsilon_X}{T_b}\right) (1 + \delta R), \quad (24)$$

where the remainder δR is defined by

$$\delta R = \frac{1-\chi}{\chi} \frac{q_N \epsilon_N}{q_X \epsilon_X} \exp\left(-\frac{\epsilon_N - \epsilon_X}{T_b}\right). \quad (25)$$

The parameter $q_X \epsilon_X / q_N \epsilon_N$ in neon mixed with xenon is given by $q_X \epsilon_X / q_N \epsilon_N = 12.8$ in Eq. (25). The ionization energies for these gas species are given by $\epsilon_N = 21.5$ eV and $\epsilon_X = 12.2$ eV. Remember that the remainder δR in Eq. (25) is the fractional contribution from neon ionization to the plasma density. The remainder δR is much less than unity except in the range of very high electron-temperature and very low mixture ratio. The plasma contribution from neon ionization can be neglected and the plasma density is described only in terms of physical parameters of xenon gas. In this regard, the plasma density in Eq. (24) is further simplified to

$$Y(n_e, \chi) \leq 10^{27} \frac{P \tau_b}{\sqrt{\pi}} \sqrt{T_b} \eta \chi q_X \epsilon_X \exp\left(-\frac{\epsilon_X}{T_b}\right). \quad (26)$$

Comparing Eqs. (18) and (26), we note that the right-hand side of Eq. (26) is almost proportional to dn_e/dt at $t = \tau_b$. This means that most of the plasma particles are generated at breakdown.

We now find the plasma density for a specified breakdown voltage V_b . Defining the single-species temperature T_0 by

$$T_0 = \frac{\xi V_b}{2.5 \times 10^{19} \sigma_N p d}, \quad (27)$$

Eq. (9) is expressed as

$$\frac{1}{T_b} = \frac{1}{T_0} (1 + \zeta \chi) \quad (28)$$

Note from Eq. (26) that the electron breakdown-temperature T_b is close to the single-species temperature T_0 for a small value of the mixture ratio, which is typical to most of the PDP applications. Substituting Eq. (26) into Eq. (24) and eliminating the breakdown temperature T_b , we approximately obtain

$$Y(n_e, \chi) \leq 10^{27} \frac{P \tau_b}{\sqrt{\pi}} \sqrt{T_0} \eta \chi q_X \epsilon_X \exp\left[-\frac{\epsilon_X}{T_0} (1 + \zeta \chi)\right], \quad (29)$$

which is the expression of plasma density for a fixed

voltage.

Note from Eq. (29) that the plasma density is described in terms of the gas mixture ratio χ . It is often very useful to find the optimum mixture ratio, at which the plasma density in Eq. (29) has its maximum value. From the differential equation of

$$\frac{\partial}{\partial \chi} Y(n_e, \chi) = 0, \quad (30)$$

we obtain

$$\chi = \chi_m = \frac{T_0}{\zeta}. \quad (31)$$

Equation (31) is obtained assuming that the relative ratio ζ of scattering cross sections is independent of the mixture ratio χ . As shown in Eq. (10), the relative ratio ζ for a specified breakdown voltage is a function of breakdown temperature T_b , which is also a function of the mixture ratio in Eq. (28). This means that the relative ratio ζ in Eq. (29) is a function of the mixture ratio χ . The corrections of the optimum mixture ratio χ_m associated with the variation of ζ in terms of χ is on the order of χ , which is typically much less than unity. We therefore neglected this contribution. The plasma density for a given breakdown voltage has its maximum value at the mixture ratio $\chi = \chi_m$ satisfying Eq. (31). Equation (31) can also be obtained from Eq. (18) by neglecting contribution of species N and by finding the optimum value of χ for maximum plasma-density increase at $T = T_b$. As an example, we consider plasma generation in neon gas mixed with xenon. The relative ratio ζ of scattering cross section in neon gas mixed with xenon is $\zeta = 11$ for the parameters identical to Fig. 2. Typical value of the single-species temperature T_0 in this mixed gas is calculated to be $T_0 = 3.9$ eV from Eqs. (14) and (15). The ionization energy of xenon is $\epsilon_X = 12.2$ eV. Substituting these numbers into Eq. (31), we find that the optimum value of mixture ratio for highest plasma density is $\chi_m = 0.03$ for neon gas mixed with xenon.

V. Conclusions

Electrical discharge properties in a mixed gas were investigated in this article. Properties of breakdown voltage in a mixed gas were investigated in Sec. II based on Townsend criterions. The breakdown

temperature T_b [Eq. (6)] and voltage V_b [Eq. (10)] were obtained in terms of the gas mixture ratio χ in Sec. II. As an example, we investigated electrical breakdown properties in neon gas mixed with xenon. It was shown that the electron breakdown-temperature T_b decreases monotonically as the mixture ratio χ increases. On the other hand, the breakdown voltage decreases, reaches the minimum value at $\chi = 0.02$ and then increases again, as the mixture ratio χ increases from zero to unity. The collision frequency of electrons by neutrals increases drastically as the mixture ratio χ increases from zero to unity. Therefore, mixing the neon gas with a few percent of xenon is the most beneficial to reduce the breakdown voltage.

Properties of plasma density at breakdown in a mixed gas were investigated in Sec. III based on the electron rate-equation. The estimate of ion density was carried out and was shown that ions consist mostly of the heavy atoms due to low ionization energy and large ionization cross-section. An expression of plasma density [Eq. (29)] was obtained in terms of the gas mixture ratio. It was also found from Eq. (29) that the maximum plasma density occurs at the mixture ratio $\chi = \chi_m = T_0/\zeta\epsilon_\chi$ [Eq. (31)]. As an example, we considered plasma generation in neon gas mixed with xenon and found that the optimum value of mixture ratio for highest plasma density is $\chi_m = 0.03$ for neon gas mixed with xenon.

Acknowledgment

This work has been supported by the G7 PDP project of the Korean Government during 1999-2000. This work was also partially supported by Grant #1999-2-112-004-3 from the Interdisciplinary

Research Program of the KOSEF.

References

- [1] H. G. Slottow, and W. D. Petty, IEEE Trans. Electron Devices **ED-2**, 650 (1970).
- [2] L. F. Weber, IEEE Trans. Electron Devices **ED-24**, 864 (1987).
- [3] G. S. Cho, Y. G. Kim, Y. S. Kim, D. G. Joh, E. H. Choi, Jpn. J. Appl. Phys. **37**, L1178 (1998).
- [4] M. J. Druyvesteyn and F. M. Penning, Rev. Modern Phys. **12**, 87 (1940).
- [5] A. M. Howatson, *An Introduction to Gas Discharges* (Pergamon Press, 1965), Chap. 3.
- [6] D. Rapp and P. J. Englander-Golden, J. Chem. Phys. **43**, 1464 (1965).
- [7] Ya. B. Zeldovich and Yu. P. Raizer, *Physics of Shock Waves and High-Temperature Hydrodynamic Phenomena* (Academic Press, New York, 1966) page 388.
- [8] E. Nasser, *Fundamentals of Gaseous Ionization and Plasma Electronics* (Wiley-Interscience, 1971) Chap. and the references therein.
- [9] R. S. Sigmond, J. Appl. Phys. **56**, 1355 (1984).
- [10] H. S. Uhm, Phys. Plasmas **6**, 4366 (1999).
- [11] Yu. P. Raizer, *Gas Discharge Physics* (Springer-Verlag, Berlin, 1997), PP. 50-100.
- [12] N. A. Krall and A. W. Trivelpiece, *Principles of Plasma Physics* (McGraw Hill, New York, 1973) Chaps. 1 and 6.
- [13] P. M. Davidson, Proc. Phys. Soc. **B**, **67**, 159 (The Physical Society, London, 1954).
- [14] A. Salop and H. H. Nakano, Phys. Rev. A **2**, 127 (1970).
- [15] C. Ramsauer, Ann. Physique **72**, 345 (1923).
- [16] J. D. Jackson, *Classical Electrodynamics* (Wiley & Sons, New York, 1962) Chap. 4.
- [17] H. S. Uhm, and W. M. Lee, Phys. Plasmas **4**, 3117 (1997); S. T. Chun (private communication 1997).
- [18] H. S. Uhm, Phys. Plasmas **6**, 4384 (1999).